

Constant and decreasing periods of pineapple slices dried by infrared

Fernanda Machado Baptestini¹, Paulo Cesar Corrêa¹, Gabriel Henrique Horta de Oliveira²,
Luís Fernando Januário Almeida¹, Guillermo Asdrúbal Vargas-Elías³

¹ Universidade Federal de Viçosa, Centro de Ciências Agrárias, Departamento de Engenharia Agrícola, Campus Universitário, CEP 36571-000, Viçosa-MG, Brasil. Caixa Postal 270. E-mail: fbaptestini@yahoo.com.br; copace@ufv.br; luis.almeida@ufv.br

² Instituto Federal do Sudeste de Minas Gerais, Campus Manhuaçu, BR 116, km 589,3, Distrito Realeza, CEP 36905-000, Manhuaçu-MG, Brasil. E-mail: gabriel.oliveira@ifsudestemg.edu.br

³ Universidad de Costa Rica, Centro para Investigaciones en Granos y Semillas, Contiguo Facultad Ciencias Agroalimentarias, San Pedro, Costa Rica. Caixa Postal 115012060. E-mail: gvargase@gmail.com

RESUMO

The aim of the present study is to model the dehydration process of pineapple slices through infrared drying, as well as to determine the critical moisture content and the critical time to the dehydration process. Pineapple slices were cut 5.0 mm thick and 2.0 cm diameter, and dried by an infrared heating source equipped with a built-in scale at accuracy of 0.001 g, under the temperatures of 50, 60, 70, 80, 90 and 100 °C, until constant weight was reached. Mass variation readings were taken at 1.0 min intervals. The mathematical models met the experimental data. The modified model by Henderson and Pabis best represented the data about the drying process. The higher drying temperature led to higher critical moisture content (from 2.205 to 2.450 kgw kg_{dm}⁻¹) and to decreased critical time (18.00 to 5.99 min). The coefficient of effective diffusion increased due to temperature (2.848 x 10⁻¹⁵ to 1.439 x 10⁻¹⁴). The activation energy of the drying process was 33.632 kJ mol⁻¹.

Palavras-chave: *Ananas comosus* L. Merril., critical moisture content, critical time, dehydration, mathematical modeling

Período constante e decrescente da secagem por infravermelho de fatias de abacaxi

ABSTRACT

O objetivo do presente trabalho foi de modelar o processo de desidratação de fatias de abacaxi secadas por infravermelho, bem como determinar o teor de água crítico e o tempo crítico para o processo de desidratação. Fatias de abacaxi foram cortadas com 5,0 mm de largura e 2,0 cm de diâmetro e secadas com uma balança de infravermelho com precisão de 0,001 g, nas temperaturas de 50, 60, 70, 80, 90 e 100 °C, até massa constante. Leituras da variação de massa foram obtidas em intervalos de 1,0 minuto. Modelos matemáticos foram ajustados aos dados experimentais. Henderson e Pabis Modificado foi o modelo que melhor representou os dados de secagem. Maiores temperaturas de secagem levaram a maiores valores de teor de água crítico (2,205 a 2,450 kgw kg_{dm}⁻¹) e decresceram o tempo crítico (18,00 a 5,99 min). O coeficiente de difusão efetivo aumentou com o incremento de temperatura (2,848 x 10⁻¹⁵ a 1,439 x 10⁻¹⁴) e a energia de ativação para o processo de secagem foi de 33,632 kJ mol⁻¹.

Key words: *Ananas comosus* L. Merril, teor de água crítico, tempo crítico, desidratação, modelagem matemática

Introduction

The pineapple fruit is widely accepted by consumers because of its taste and aroma. It is rich in sugars, minerals and vitamins and can be consumed either fresh or industrialized in slices or pieces within syrup, in dehydrated jellies, etc.

One of the factors that impair fresh pineapple consumption is its inconvenient peeling process, which is tiring and requires proper equipment given the liquid leak and the difficulty to reduce the pieces. Another obstacle to its consumption is consumers' resistance to substances used to preserve processed food.

A way to overcome the aforementioned difficulties may be the fruit dehydration process. According to Ramos et al. (2008), the increased popularity of high quality dehydrated meals that can be quickly prepared has led to the considerable increase in the interest for dehydrated products.

Dehydration extends the shelf life of food by removing part of the water, thereby reducing microbiological deterioration and degradation reactions. It allows the constant availability of seasonal food. In addition, it reduces the mass and volume of the product by increasing transportation and storage efficiency. It also aggregates value to foods, since a product with chemical and physical properties different from the fresh product is available in the market.

According to Hebbar & Rastoge (2001), the infrared drying process offers significant advantages in comparison to the conventional drying methods. When infrared radiation is used to heat or dry moist materials the radiation penetrates the exposed material and radiation is converted into heat. The radiation penetration depth depends on the properties of the material and on the wavelength. When the material is exposed to radiation, it is intensely heated and the temperature gradient in the material reduces within a short period.

The agricultural products such as fruits and vegetables have high moisture content besides other components such as vitamins, carbohydrates, protein, fiber and minerals. When these moist materials are subjected to the drying process they present their own drying curves. Usually, these curves are characterized by constant and decreasing drying rates.

Weight changes are constant in the constant drying rate period. Such process takes place because the internal water displacement rate to the product surface is equal or greater than the maximum water vapor removal by the air, since just the free water is evaporated (Celestino, 2010). On the other hand, during the decreasing drying rate period the amount of water found on the product surface is lower, thus the mass transference is reduced. The process ends when the product reaches the moisture equilibrium point in comparison to the air drying (Brooker et al., 1992).

The moisture content is defined as critical when the constant drying rate becomes the decreasing drying rate period. According to Brooker et al. (1992), the critical moisture content is extremely difficult to be determined and it depends on the drying conditions and on product features such as shape and granulometry.

In light of the foregoing, the aim of the present study is to obtain and model the pineapple slice drying curves in

experiments at temperatures ranging from 50 to 100 °C in order to determine the critical moisture content and the critical time, as well as the effective diffusion coefficient. The results will enable better understanding and controlling the dehydration process, which determines the quality of the final product offered to the consumers.

Material and Methods

The current study was conducted in the Laboratory of Physical Properties and Quality of Agricultural Products at Federal University of Viçosa. The pineapple fruits used in the experiment were bought in the local market and stored in a BDO chamber at 25 ± 1 °C throughout the experiment. The slices were cut approximately 5.0 mm thick and 2.0 cm diameter. An infrared dryer equipped with a built-in scale (0.001 g precise) operating at the temperatures of 50, 60, 70, 80, 90 and 100 °C was used to dry the material. The dryer provided information about mass variation at 1 min intervals. The pineapple slices were dried up to constant mass. Mathematical models met the experimental data (Table 1).

Table 1. Mathematical models used to describe the drying process

Model name	Model	
Approximation of diffusion	$MR = a \exp(-kt) + (1 - a)\exp(-kbt)$	(1)
Two terms	$MR = a \exp(-k_0t) + b \exp(-k_1t)$	(2)
Henderson & Pabis	$MR = a \exp(-kt)$	(3)
Logarithmic	$MR = a \exp(-kt) + b$	(4)
Midilli	$MR = a \exp(-kt^n) + bt$	(5)
Newton	$MR = \exp(-kt)$	(6)
Page	$MR = \exp(-kt^n)$	(7)
Verma	$MR = a \exp(-kt) + (1 - a)\exp(-k_1t)$	(8)
Copace	$MR = (a + bt)/(1 + ct + dt^2)$	(9)
Modified Henderson & Pabis	$MR = a \exp(-kt) + b \exp(-k_0t) + c \exp(-k_1t)$	(10)

Where: MR: Moisture Ratio, dimensionless; t: drying time, min; k, k_0 , k_1 : drying constant, min^{-1} ; a, b, c, d, n: model coefficients, dimensionless.

The moisture ratio was determined according to Equation 11. The simplification results from the infrared drying, the samples can be dried up to constant dry matter ($M_e=0$) (Toğrul, 2006).

$$MR = \frac{M_t - M_e}{M_0 - M_e} \cong \frac{M_t}{M_0} \quad (11)$$

where: M_t - moisture content at a time t, $\text{kg}_w \text{kg}_{\text{dm}}^{-1}$; M_0 - initial moisture content, $\text{kg}_w \text{kg}_{\text{dm}}^{-1}$; M_e - moisture content in equilibrium, $\text{kg}_w \text{kg}_{\text{dm}}^{-1}$.

Equation 12 was used to determine the binomial critical moisture content and the critical time. This equation was adapted from Stupa et al. (2003) and Reis et al. (2013), who describe the constant rate periods and the decreasing rate, separated by the critical time.

$$M_t = [M_0 - (c \times t)] \times (t \leq t_c) + \{M_c \times \exp[k \times (t - t_c)]\} \times (t > t_c) \quad (12)$$

where: M_c - critical moisture content, $\text{kg}_w \text{kg}_{\text{dm}}^{-1}$; c - drying rate in constant period, min^{-1} ; k - drying rate in decreasing period, min^{-1} ; t_c - critical time, min.

The experimental data of pineapple slices drying were subjected to non-linear regression analysis. The model that best represented the relationship between the studied variables was selected.

The magnitude of determination coefficient, the mean relative percent deviation (P) (Equation 13), the standard error (SE) (Equation 14), the residual distribution (RD) and the residual cumulative frequency (RCF) were taken into account to analyze the degree of fit to each model.

$$P = \frac{100}{n_{obs}} \sum_{i=1}^{n_{obs}} \frac{|Y_i - \hat{Y}_i|}{Y_i} \quad (13)$$

$$SE = \sqrt{\frac{\sum_{i=1}^{n_{obs}} (Y_i - \hat{Y}_i)^2}{GLR}} \quad (14)$$

where: Y_i - observed value; \hat{Y}_i - estimated value; n_{obs} - number of observed data; GLR - degrees of freedom of the residue.

The effective diffusion coefficient was obtained through the matching of the liquid diffusion mathematical model, described in Equation 15, and the experimental drying curves. This equation is the analytical solution to Fick's Second Law. It takes the flat geometrical shape and the boundary condition of moisture on the surface of the product into consideration, and ignores the volumetric contraction of it.

$$\begin{aligned} MR &= \frac{M_t - M_e}{M_0 - M_e} \\ &= \frac{8}{\pi^2} \sum_{n=0}^{\infty} \frac{1}{(2n+1)^2} \exp\left[-\frac{(2n+1)^2 \pi^2 D_{ef} t}{4L^2}\right] \end{aligned} \quad (15)$$

where: L - product thickness, m; D_{ef} - effective diffusion coefficient, $m^2 s^{-1}$; n - number of equation terms.

The Arrhenius equation was used (Equation 16) to evaluate the influence of temperature on the effective diffusion coefficient (Doymaz et al., 2006; Gely & Giner, 2007; Gely & Santalla, 2007).

$$D_{ef} = D_0 \exp\left(\frac{E_a}{RT_{abs}}\right) \quad (16)$$

where: D_0 - pre-exponential factor $m^2 s^{-1}$; E_a - activation energy, $kJ mol^{-1}$; T_{abs} - absolute temperature K.

Results and Discussion

Figure 1 shows the observed and estimated values of pineapple slice drying curves at temperatures ranging from 50 to 100 °C. The figure below shows the distinct drying periods, the constant rate and the decreasing rate. The free water evaporation process occurs at constant pressure during the period of constant rate due to the high amount of water molecules (Park et al., 2007). The temperature of the product

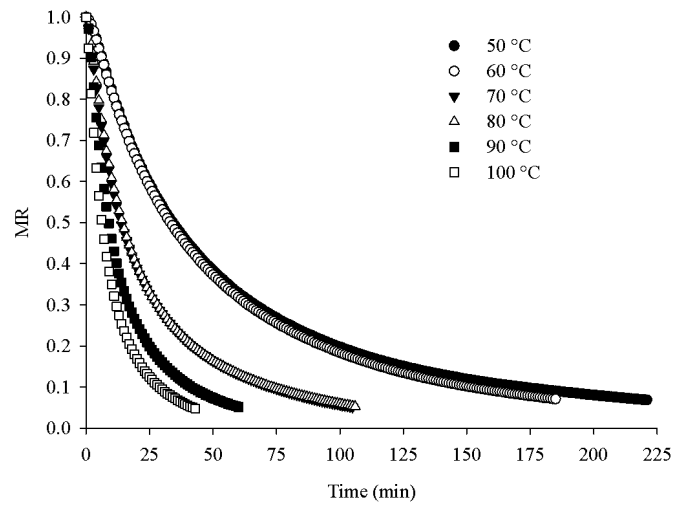


Figure 1. Experimental and estimated values of pineapple slice drying curves at temperatures ranging from 50 to 100 °C

is constant and equals to the wet bulb temperature, since the heat and mass transference are compensated. Furthermore, this drying period depends only on the external conditions of the process (speed, temperature and relative air humidity) (Brooker et al., 1992).

The heat transfer is compensated by the mass transfer at the decreasing rate period in the drying periods (Figure 1), because the internal resistance to moisture transportation becomes stronger than the external resistance (Brooker et al., 1992). Such factor limits the reduction in water molecule migration from the interior to the surface of the product. Thus, the temperature increases and may reach the air-drying temperature.

The effect of the drying temperature can also be seen in Figure 1. The drying time decreases and the curves acquire a greater inclination as the temperature increases due to a larger amount of heat transferred from the air to the material. Consequently, there is increase in the water migration speed from the product to the surface.

Table 2 shows the R^2 (determination coefficient), SE (standard error), P (mean relative percent deviation), RD (residual distribution) and RCF (residual cumulative frequency) values of pineapple slices at temperatures ranging from 50 to 100 °C.

According to the results in Table 2, the modified Henderson and Pabis model better represents the pineapple slice drying process. It presents R^2 values higher than 99.99%, P below 1.039, SE below 0.0012, random residue distribution (Figure 2a) and normal distribution of residual frequency (Figure 2b) in all the drying conditions in comparison to the other models. The model ability to accurately describe a physical process is inversely proportional to the SE values (Draper & Smith, 1998). Furthermore, models using P values below 10% are the most suitable for predicting the phenomena (Mohapatra & Rao, 2005). Hence, only Newton and Henderson and Pabis' models are inadequate for describing the drying rate of pineapple slices.

Table 3 shows the estimated parameters of Henderson and Pabis' modified drying model of pineapple slices at temperatures ranging from 50 to 100 °C.

Table 2. Determining the coefficient (R^2), standard error (SE), mean relative percent deviation (P), residual distribution (RD) and residual cumulative frequency (RCF) of pineapple slices at temperatures ranging from 50 to 100 °C

Model	P	SE	R^2	RD	RCF	P	SE	R^2	RD	RCF
50 °C										
Approximation of diffusion	0.67	0.006	99.9	R	NN	1.06	0.006	99.9	R	NN
Two terms	0.81	0.003	99.9	R	NN	0.46	0.003	99.9	R	NN
Henderson & Pabis	19.32	0.033	97.9	B	NN	14.01	0.027	98.7	B	NN
Logarithmic	5.53	0.011	99.8	B	NN	4.79	0.010	99.8	B	NN
Midilli	2.64	0.007	99.9	B	NN	2.21	0.007	99.9	R	NN
Newton	24.54	0.039	97.2	B	NN	17.60	0.031	98.3	B	NN
Page	8.37	0.018	99.4	B	NN	5.72	0.015	99.6	B	NN
Verma	0.67	0.006	99.9	R	NN	1.06	0.006	99.9	R	NN
Copace	0.58	0.003	99.9	R	NN	0.83	0.004	99.9	R	NN
Modified Henderson & Pabis	1.04	0.002	99.9	R	N	0.51	0.001	99.9	R	N
70 °C										
Approximation of diffusion	1.09	0.005	99.9	R	NN	1.41	0.007	99.9	R	NN
Two terms	0.44	0.003	99.9	B	NN	0.49	0.004	99.9	B	NN
Henderson & Pabis	23.82	0.036	97.5	B	NN	24.15	0.036	97.6	B	NN
Logarithmic	10.04	0.016	99.5	B	NN	9.16	0.014	99.6	B	NN
Midilli	4.78	0.010	99.8	B	NN	4.87	0.011	99.8	B	NN
Newton	31.03	0.043	96.4	B	NN	29.97	0.040	96.9	B	NN
Page	8.53	0.017	99.4	B	NN	9.82	0.019	99.3	B	NN
Verma	1.09	0.005	99.9	R	NN	1.08	0.008	99.9	R	NN
Copace	2.08	0.005	99.9	R	NN	2.31	0.005	99.9	R	NN
Modified Henderson & Pabis	0.49	0.001	99.9	R	N	0.62	0.001	99.9	R	N
90 °C										
Approximation of diffusion	2.78	0.012	99.8	R	NN	1.51	0.007	99.9	R	NN
Two terms	1.71	0.008	99.9	B	NN	0.91	0.006	99.9	B	NN
Henderson & Pabis	22.04	0.032	98.4	B	NN	21.86	0.030	98.5	B	NN
Logarithmic	7.96	0.013	99.7	B	NN	8.25	0.013	99.7	B	NN
Midilli	5.77	0.013	99.7	B	NN	4.91	0.011	99.8	B	NN
Newton	24.64	0.033	98.2	B	NN	25.92	0.033	98.2	B	NN
Page	10.67	0.022	99.2	B	NN	8.80	0.017	99.5	B	NN
Verma	3.81	0.008	99.9	R	NN	1.51	0.007	99.9	R	NN
Copace	2.77	0.012	99.8	R	NN	2.42	0.006	99.9	R	NN
Modified Henderson & Pabis	0.53	0.001	99.9	R	N	0.67	0.001	99.9	R	N
100 °C										
Approximation of diffusion	2.78	0.012	99.8	R	NN	1.51	0.007	99.9	R	NN
Two terms	1.71	0.008	99.9	B	NN	0.91	0.006	99.9	B	NN
Henderson & Pabis	22.04	0.032	98.4	B	NN	21.86	0.030	98.5	B	NN
Logarithmic	7.96	0.013	99.7	B	NN	8.25	0.013	99.7	B	NN
Midilli	5.77	0.013	99.7	B	NN	4.91	0.011	99.8	B	NN
Newton	24.64	0.033	98.2	B	NN	25.92	0.033	98.2	B	NN
Page	10.67	0.022	99.2	B	NN	8.80	0.017	99.5	B	NN
Verma	3.81	0.008	99.9	R	NN	1.51	0.007	99.9	R	NN
Copace	2.77	0.012	99.8	R	NN	2.42	0.006	99.9	R	NN
Modified Henderson & Pabis	0.53	0.001	99.9	R	N	0.67	0.001	99.9	R	N

Note: R: random; B: biased; N: normal; NN: non-normal.

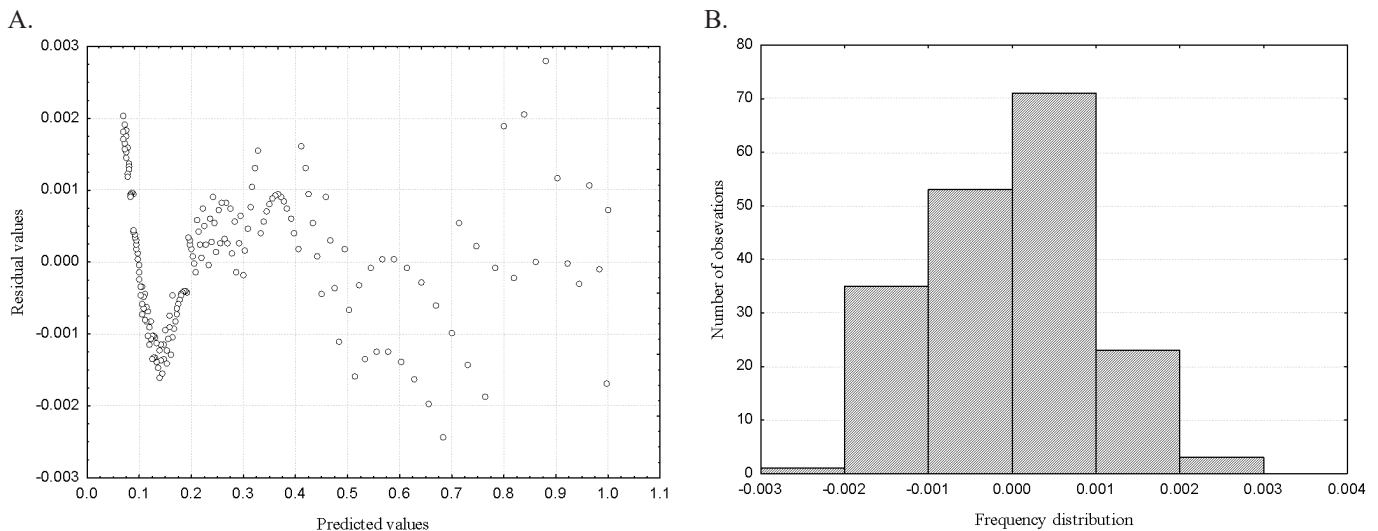
**Figure 2.** Distribution of residues (A.) and residual frequency (B.) of the modified Henderson and Pabis model at 60 °C

Table 4 presents the estimated parameters of the fitted model (Equation 12), its respective determination coefficients (R^2), standard error (SE) and mean relative percent deviation (P) at temperatures ranging from 50 to 100 °C.

Table 4 shows the effect of the drying temperature on the estimated parameters. The estimated values of the critical moisture content are inserted within the range suggested by Brooker et al. (1992) such as the transition values from the constant rate period to the decreasing rate period (2.333 to 3.000 $\text{kg}_w \text{kg}_{dm}^{-1}$). It can be concluded that the adapted model

met the experimental data. However, this effect is evidenced in Figures 3 and 4 for the better comprehension of the process.

The parameter c (Figure 3a) represents the drying rate during the constant period. The temperature increases as the drying rate increases. On the other hand, the parameter k (Figure 3b), which represents the drying rate during the decreasing period, decreases as the temperature increases; values range from -0.013 to -0.071.

The effect of the drying temperature on the critical time can be seen in Figure 4a. The increased temperature results in

Table 3. Estimated parameters of Henderson and Pabis' modified drying model of pineapple slices at temperatures ranging from 50 to 100 °C

Parameters	Temperature (°C)					
	50	60	70	80	90	100
a	0.63958	0.52247	0.59557	0.42964	0.47109	0.47270
k	0.03427	0.04088	0.09435	0.02000	0.03736	0.05410
b	0.40153	0.52862	0.45097	0.63330	0.65302	0.59088
k ₀	0.00819	0.01103	0.02076	0.08880	0.15529	0.21011
c	-0.04226	-0.05182	-0.04671	-0.06316	-0.12418	-0.06358
k ₁	0.78672	0.59952	1.55679	1.12063	1.12045	3.24675

Table 4. Estimated parameters of the fitted model (Equation 12), its respective determination coefficients (R²), standard error (SE) and mean relative percent deviation (P) at temperatures ranging from 50 to 100 °C

Parameters	Temperature (°C)					
	50	60	70	80	90	100
t _c	18.00	18.19	12.86	13.05	8.00	5.99
M _c	2.243	2.205	2.304	2.238	2.370	2.450
c	0.067	0.066	0.194	0.181	0.302	0.464
k	-0.013	-0.015	-0.027	-0.027	-0.048	-0.071
P	10.895	6.988	8.422	8.601	7.397	8.002
SE	0.069	0.048	0.066	0.066	0.061	0.062
R ²	99.32	99.66	99.64	99.65	99.76	99.78

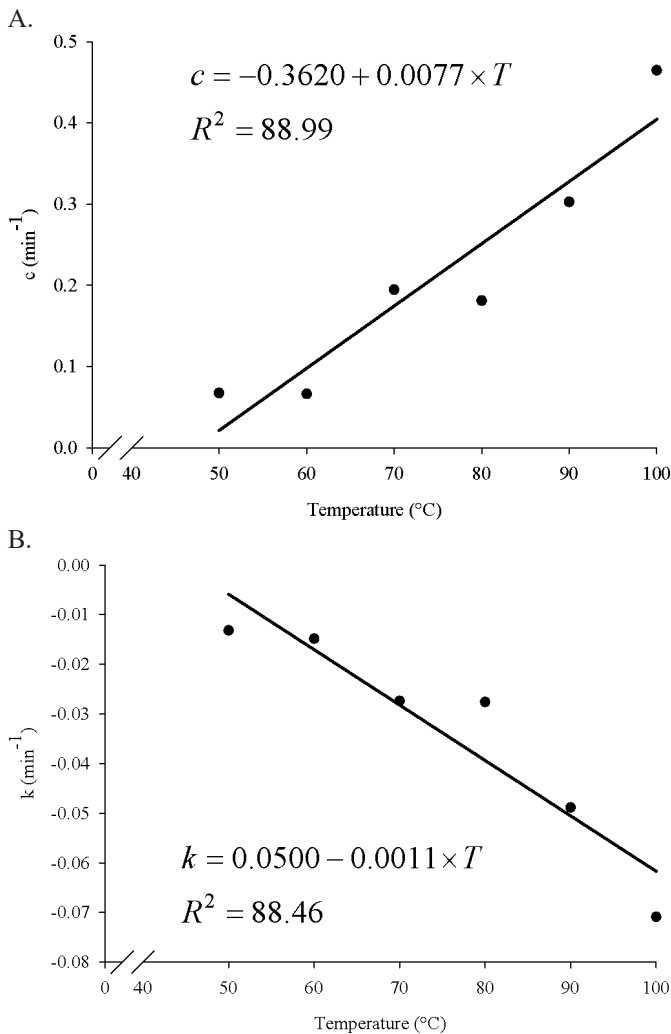


Figure 3. Effect of the drying temperature in parameters c (A.) and k (B.), as well as the regression equation of the mean results according to temperature (T), and its determination coefficient

critical time decrease. Such fact and the critical moisture content represent the transition point between the different drying stages.

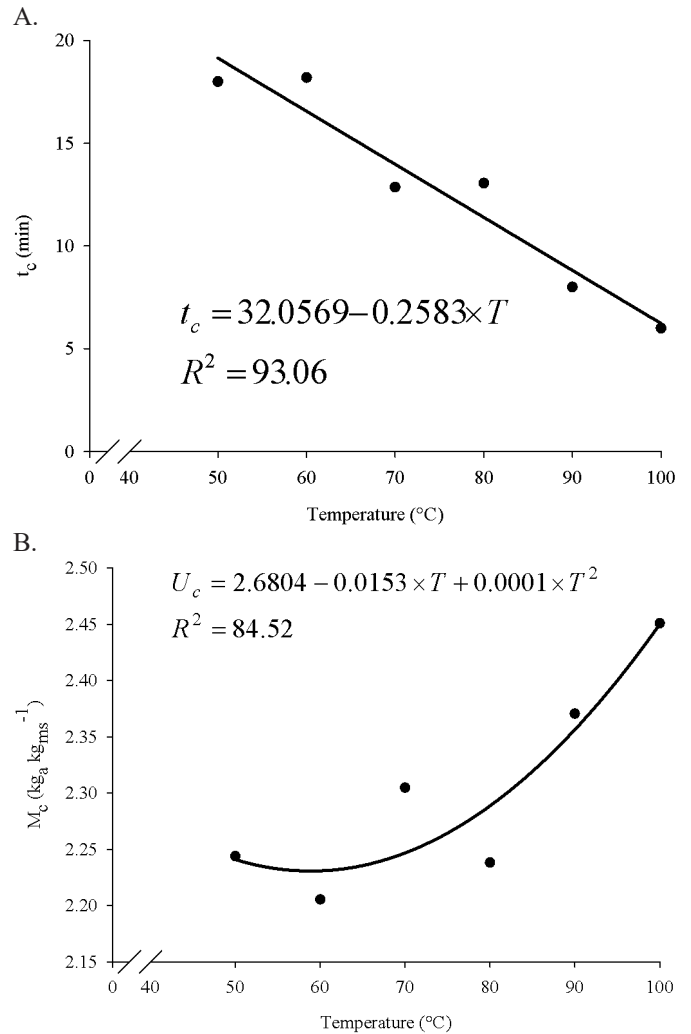


Figure 4. Effect of the drying temperature on parameters t_c (A.) and M_c (B.) as well as the regression equation of the mean results according to the temperature (T) and its coefficient of determination

The critical moisture content (Figure 4b) is that when the water coating layer decreases and the temperature on the surface of the product starts to increase, so it tends to match the external temperature, or also when the water migration to the surface of the product can no longer meet the evaporated free water and the temperature of the material increases and tends to match the air drying temperature (Chirife, 1987). The drying curve decreases exponentially from the critical moisture content on.

The effect of temperature on the critical moisture content was the same of that found by Reis et al. (2013) and Waje et al. (2005). It means that M_c increased as the drying temperature also increased. On the other hand, Stupa et al. (2003) found different results. Such trend demonstrates that many studies are required in order to find further information on the subject, since the critical moisture content is difficult to be set and depends on the drying conditions and on product features such as shape and texture, fact that would probably interfere in the results (Brooker et al., 1992).

Table 5 shows the effective diffusion coefficients of pineapple slices dried at 50, 60, 70, 80, 90 and 100 °C.

Table 5 shows that the effective diffusion coefficients of pineapple slices increased as the temperature increased;

Table 5. Effective diffusion coefficients of pineapple slices dried at the temperatures of 50, 60, 70, 80, 90 and 100 °C, as well as the regression equation of the mean results according to the temperature (T), and its determination coefficient

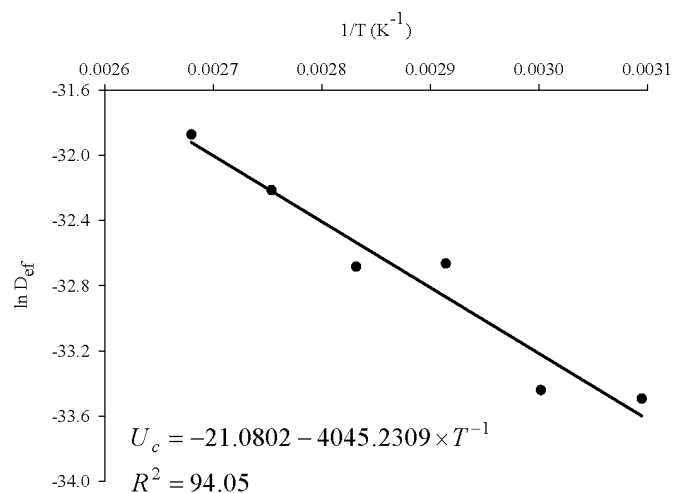
Temperature (°C)					
50	60	70	80	90	100
2.848×10^{-15}	3.001×10^{-15}	6.518×10^{-15}	6.399×10^{-15}	1.022×10^{-14}	1.439×10^{-14}
$D_{ef} = -9.7569 \times 10^{-15} + 2.2265 \times T$					$R^2 = 91.09$

therefore, it presented a linear correlation with the drying temperature.

As there are several possible moisture transportation mechanisms in porous products such as liquid movement due to surface forces (capillary diffusion), liquid movement due to moisture diffusion on pores surfaces (surface diffusion), liquid and steam movement due to total pressure difference caused by external pressure, shrinkage, high temperature and capillary (hydrodynamic flow) and steam movement due to temperature differences (thermal diffusion) (Brooker et al., 1992), the liquid diffusion is better represented as effective diffusion coefficient.

The effective diffusion coefficient variation according to the drying temperature is described through the Arrhenius relationship (Figure 5).

The activation energy of water diffusion in pineapple slices and the drying process based on the studied temperature range was 33.632 kJ mol⁻¹. The lower the activation energy in the drying process was, the greater the water diffusivity in the product. Toğrul (2006) and Botelho et al. (2011) found activation energy values of 22.43 and 29.09 kJ mol⁻¹ when they infrared dried carrots at temperatures ranging from 50 to 80 °C and from 50 to 100 °C, respectively. However, values outside this range can also be found, as it was observed by Reis et al. (2011) when they studied the convective drying of *Cumari do Para* pepper and found activation energy of 5.7 kJ mol⁻¹.

**Figure 5.** Arrhenius representation of pineapple slices at different drying temperatures, as well as the regression equation of the mean results according to the temperature (T) and its coefficient of determination

Conclusions

The results show that there is an inverse relationship between temperature and drying time.

The modified Henderson and Pabis model was the one that better met the experimental data about pineapple drying.

The increase in the drying temperature leads to increase in the critical moisture content from 2.205 to 2.450, and decrease in critical time from 18.00 to 5.99.

The effective diffusion coefficient increased as the temperature increased and such association can be represented by the Arrhenius equation, which showed 33.632 kJ mol⁻¹ of activation energy in the drying process.

Acknowledgements

The authors thank CNPq for the financial support.

Literature Cited

- Botelho, F.M.; Corrêa, P.C.; Goneli, A.L.D.; Martins, M.A.; Magalhães, F.E.A.; Campos, S.C. Periods of constant and falling-rate for infrared drying of carrot slices. *Revista Brasileira de Engenharia Agrícola e Ambiental*, v.15, n.8, p.845-852, 2011. <<http://dx.doi.org/10.1590/S1415-43662011000800012>>.
- Brooker, D.B.; Bakker-Arkema, F.W.; Hall, C.H. *Drying and storage of grains and oilseeds*. Westport: The AVI Publishing Company, 1992. 450p.
- Celestino, S.M.C. *Princípios de secagem de alimentos*. Planaltina: Embrapa Cerrados, 2010. 51p. (Documentos. Embrapa Cerrados, 276). <<http://www.cpac.embrapa.br/download/1735/t>>. 22 Jun. 2014.
- Chirife, J. *Fundamentals of the drying mechanism during air of foods*. In: Mujumdar, A.S. (Ed.) *Advances in drying*. Washington: Hemisphere Publishing Corporation, 1987. p. 73-102.
- Doymaz, I.; Tugrul, N.; Pala, M. Drying characteristics of dill and parsley leaves. *Journal of Food Engineering*, v.77, n.3, p.559-565, 2006. <<http://dx.doi.org/10.1016/j.jfoodeng.2005.06.070>>.
- Draper, N.R.; Smith, H. *Applied regression analysis*. New York: John Wiley & Sons, 1998. 712p.
- Gely, M.C.; Giner, S.A. Diffusion coefficient relationships during drying of soya bean cultivars. *Biosystems Engineering*, v.96, n.2, p.213-222, 2007. <<http://dx.doi.org/10.1016/j.biosystemseng.2006.10.015>>.
- Gely, M.C.; Santalla, E.M. Moisture diffusivity in quinoa (*Chenopodium quinoa* Willd.) seeds: Effect of air temperature and initial moisture content of seeds. *Journal of Food Engineering*, v.78, n.3, p.1029-1033, 2007. <<http://dx.doi.org/10.1016/j.jfoodeng.2005.12.015>>.
- Hebbbar, H.U.; Rastogi, N.K. Mass transfer during infrared drying of cashew kernel. *Journal of Food Engineering*, v.47, n.1, p.1-5, 2001. <[http://dx.doi.org/10.1016/S0260-8774\(00\)00088-1](http://dx.doi.org/10.1016/S0260-8774(00)00088-1)>.

- Mohapatra, D.; Rao, P.S. A thin layer drying model of parboiled wheat. *Journal of Food Engineering*, v.66, n.4, p.513-518, 2005. <<http://dx.doi.org/10.1016/j.jfoodeng.2004.04.023>>.
- Park, K.J.; Antonio, G.C.; Oliveira, R.A.; Park, K.J.B. *Conceitos de processos e equipamentos de secagem*. Campinas: Unicamp, 2007. 121p.
- Ramos, A.M.; Quintero, A.C.F.; Faraoni, A.S.; Soares, N.F.F.; Pereira, J.A.M. Efeito do tipo de embalagem e do tempo de armazenamento nas qualidades físico-química e microbiológica de abacaxi desidratado. *Alimentos e Nutrição*, v.19, n.3, p.259-269, 2008. <<http://serv-bib.fcfar.unesp.br/seer/index.php/alimentos/article/viewFile/629/527>>. 22 Jun. 2014.
- Reis, R.C.; Barbosa, L.S.; Lima, M.L.; Reis, J.S.; Devilla, I.A.; Ascheri, D.P.R. Modelagem matemática da secagem da pimenta Cumari do Pará. *Revista Brasileira de Engenharia Agrícola e Ambiental* 2011, v.15, n.4, p.347-353, 2011. <<http://dx.doi.org/10.1590/S1415-43662011000400003>>.
- Reis, R.C.; Côrrea, P.C.; Devilla, I.A.; Santos, E.S.; Ascheri, D.P.R.; Servulo, A.C.O.; Souza, A.B.M. Drying of yam starch (*Discorea* ssp.) and glycerol filmogenic solutions at different temperatures. *Food Science and Technology*, v.50, n.2, p.651-656, 2013. <<http://dx.doi.org/10.1016/j.lwt.2012.07.033>>.
- Stupa, M.V.; Platonov, E.K.; Milkhailov, V.T. Mathematical model of drying of granulated anid. *Fibre Chemistry*, v.35, n.3, p.233-236, 2003. <<http://dx.doi.org/10.1023/A:1026174310080>>.
- Toğrul, H. Suitable drying model for infrared drying of carrot. *Journal of Food Engineering*, v.77, n.3, p.610-619, 2006. <<http://dx.doi.org/10.1016/j.jfoodeng.2005.07.020>>.
- Waje, S.S.; Meshram, M.W.; Chaudhary, V.; Pandey, R.; Mahanawar, P.A.; Thorat, B.N. Drying characteristics of hydrophilic polymer gel: co-polymer of acrylic acid and acrylamide. *Brazilian Journal of Chemical Engineering*, v.22, n.2, p.209-216, 2005. <<http://dx.doi.org/10.1590/S0104-66322005000200007>>.